Light-Scattering and Ellipsometry Studies of the Two-Dimensional Smectic-C to Smectic-A Transition in Thin Liquid-Crystal Films

Light-scattering and ellipsometry studies of the two-dimensional smectic-C to smectic-A transition in thin liquid-crystal films

S. M. Amador*
Division of Applied Sciences, Harvard University, Cambridge, Massachusetts 02138

P. S. Pershan
Department of Physics and Division of Applied Sciences, Harvard University, Cambridge, Massachusetts 02138
(Received 20 November 1989)

Ellipsometry and light-scattering measurements are presented for the critical region near the two-dimensional *XY*-like smectic-*C* to smectic-*A* phase transition in thin, freely suspended films of the liquid crystal *p*-decyloxybenzylidene *p*-aminocinnamaic acid 2-methylbutyl ester. The macroscopically observed smectic-*C* tilt order parameter was found to obey a scaling relation as a function of temperature and film thickness, indicating that only the surface layers order over a wide range of temperatures. Deep within the smectic-*C* phase, the tilt order parameters for all thickness films measured converged upon a unique value at which the smectic-*C* to smectic-*I* transition took place. The light-scattering intensities and decay times above the smectic-*C* to smectic-*A* transition were found to scale with the Kosterlitz-Thouless correlation length, as predicted by dynamical theories of the transition. Measurements of the predicted Nelson-Kosterlitz universal jump in θ concurred with estimates for the bulk material parameters and with the light-scattering results.

I. INTRODUCTION

The Kosterlitz-Thouless (KT) scenario of defect-mediated phase transitions in two dimensions[1] has been tested more or less directly in numerous physical systems, including two-dimensional (2D) superfluids[2–5] and proximity-coupled superconducting arrays,[6] as well as in computer simulations of the critical behavior of *XY* systems.[7] In the years since its first proposal, the widening applications of the binding-unbinding transition concept have made the question of when and where it applies an even more interesting one.

An especially direct test of the predictions of the KT model was suggested by Rosenblatt *et al.*[8–11] who studied thin, smectic-*C* (Sm-*C*) liquid-crystal films below the smectic-*C*, or tilted 2D liquid, to smectic-*A* (Sm-*A*), or 2D liquid, transition temperature. This system can be imagined as analogous to the *XY* model if the projection of the director in the plane of the layers, **c** is taken as the *XY* order parameter (see Fig. 1). Alternatively, the Sm-*C* order parameter $\theta e^{i\phi}$ can be expressed in terms of the tilt from normal (θ) and the azimuthal tilt in plane (ϕ). The evolution of the director's tilt from normal θ has been assumed to provide a smoothly varying temperature dependence which does not alter the character of the *XY* transition. However, due to experimental limitations, Rosenblatt *et al.* were unable to resolve one of the most striking predictions for the transition, the universal jump in the two-dimensional elastic constant. In a later paper, Heinekamp *et al.*[12] observed via ellipsometry the variation of θ with temperature below and close to the Sm-*C* to Sm-*A* transition temperature. Their analysis showed that a mean-field theory with effects due to enhanced surface tilts accounted for the main features of their data for θ. In this paper, we present light-scattering and ellipsometry measurements on freely suspended films of the liquid-crystal *p*-decyloxybenzylidene *p*-aminocinnamaic acid 2-methylbutyl ester, commonly abbreviated as DOBAMBC, which extend the prior results to the critical transition region.

II. THEORY

Kosterlitz and Thouless have predicted that the *XY* model will melt via a defect binding-unbinding transition.[1] This phenomenon has several peculiar features when compared to a standard second-order phase transition. The thermodynamic variables of the system scale as powers of the correlation length ξ_+ (defined as the length over which tilt order persists), but the correlation length itself does not scale as a power of the reduced temperature. Instead, its temperature dependence has an essential singularity at the transition temperature T_{XY},

$$\xi_+ = \xi_0 e^{b/|T-T_{XY}|^{1/2}} \tag{2.1}$$

for $T \to T_{XY}$ from above T_{XY} in temperature, where ξ_0 is of the order of the thickness of the film; for $T < T_{XY}$, $\xi_+ = \infty$. In addition, Nelson and Kosterlitz have predicted[13] that at the transition the 2D elastic constant K will undergo a discontinuous jump to zero in the higher temperature phase, with the universal value

$$\lim_{T \to T_{XY}} K = (2/\pi) k_B T_{XY} \ . \tag{2.2}$$

For the ferroelectric Sm-*C** phase, to lowest order in $\phi(r)$ and allowing for in-plane anisotropy,[14] one can write a Landau free energy density $F(\phi)$ in terms of fluctua-

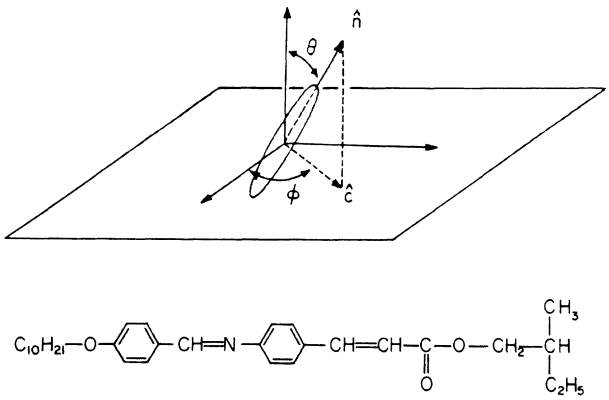

FIG. 1. Idealized rendering of the configuration of molecules in a smectic-C liquid crystal, and the chemical formula of the liquid crystal, DOBAMBC, used in this study. The rodlike molecules of a smectic liquid crystal have their centers of mass confined to planes within the material. The orientation of the molecules in the smectic-C phase can be described by a polar angle θ and an azimuthal angle ϕ, the latter of which resembles the XY degree of freedom. In the smectic-A phase, the polar angle becomes zero on average.

tions in the in-plane order parameter,

$$F=\tfrac{1}{2}K_{\perp}\left[\frac{\partial\phi}{\partial r_{\perp}}\right]^2+\tfrac{1}{2}K_{\parallel}\left[\frac{\partial\phi}{\partial r_{\parallel}}\right]^2-P_0Nh\,(\sin\theta)E_a\cos\phi$$
$$+\text{dipole-dipole terms}\ , \tag{2.3}$$

where $\mathbf{r}$ is the position within the plane; P_0 is the amplitude of the in-plane polarization of the ferroelectric liquid crystal; N the number of layers in the film; h is the thickness of an individual layer, equal to ~ 33 Å for small values of θ; E_a the amplitude of an aligning electric field; and where the $\perp$ and $\parallel$ refer to directions in the smectic plane perpendicular and parallel to the in-plane projection of the director, respectively. The 2D elastic constants, which correspond to the restoring force in response to deformations of $\phi(r)$ perpendicular to and along the direction of the average tilt, can be given in terms of the bulk splay, twist, and bend elastic constants K_{11}, K_{22}, and K_{33} as

$$K_{\perp}=NhK_{11}\sin^2\theta\ , \tag{2.4a}$$

$$K_{\parallel}=Nh\,\sin^2\theta[K_{22}\cos^2\theta+K_{33}\sin^2\theta]$$
$$=\bar{K}Nh\,\sin^2\theta\ . \tag{2.4b}$$

Far from $T_{C\text{-}A}$, the temperature evolution of θ is considered to be given by mean-field theory; however, near $T_{C\text{-}A}$ it is due to the effects of disclinations in the ordering field $\phi(r)$ and the effective $T_{C\text{-}A}$ is identified with the Kosterlitz-Thouless transition temperature T_{XY}. This analogy to KT melting should hold even in the presence of anisotropy, dipolar forces, and weak aligning electric fields for the correlation lengths we expect to probe in these measurements.[14] This expression for $F(\phi)$ allowed Rosenblatt *et al.* to solve for the spectrum of light elastically scattered from fluctuations in ϕ which give rise to fluctuations in the dielectric tensor of the material.[10,11] The universal jump value should equal

$$K^*=(2/\pi)k_BT_{XY}$$
$$=\tfrac{1}{2}(K_{\perp}+K_{\parallel})$$
$$=\tfrac{1}{2}(K_{11}+\bar{K})Nh\,\sin^2\theta^*\ , \tag{2.5}$$

where θ^* is the predicted jump in θ.

Heinekamp and Pelcovits have solved for the critical dynamics of the Sm-C to Sm-A transition including disclination effects near $T_{C\text{-}A}$.[15] They find for the autocorrelation function of the scattered electric field E_s

$$\langle E_s(\mathbf{q},\omega)E_s^*(\mathbf{q},\omega)\rangle$$
$$=\langle\tilde{\phi}(\mathbf{q},\omega)\tilde{\phi}^*(\mathbf{q},\omega)\rangle$$
$$\times\left[1-2\int\langle S(\mathbf{q}',\omega)S^*(\mathbf{q}',\omega)\rangle d^2q'\right.$$
$$\left.+3\left[\int\langle S(\mathbf{q}',\omega)S^*(\mathbf{q}',\omega)\rangle d^2q'\right]^2\right]\ , \tag{2.6}$$

where $\phi(\mathbf{q},\omega)$ is the time and spatial Fourier transform of the azimuthal angle field, and the function $S(\mathbf{q},\omega)$ is the spectral density of the free disclination field. The first term comes close to merely reproducing the spin-wave results of Rosenblatt *et al.* for $\langle E_s(\mathbf{q},t)E_s^*(\mathbf{q},0)\rangle$, while the latter two terms include the effects of free disclinations on the projected length of the director. The first term defines a characteristic length scale for $\mathbf{q}$ determined by the KT correlation length ξ_+. The hydrodynamics will be Sm-C-like for $q\xi_+\gg 1$ (length scales shorter than the correlation length) even above $T_{C\text{-}A}$, exhibit a crossover region for $q\xi_+\sim 1$, and be Sm-A-like for $q\xi_+\ll 1$. Thus the observed hydrodynamics should depend upon the length scale being measured, and hence upon the momentum-transfer vector $\mathbf{q}$. The exact expression for the first term in Eq. (2.6) in the time domain is, ignoring polarization-dependent terms, and assuming $K=K_{\perp}=K_{\parallel}$,

$$\langle E(q,t)E_s^*(q,0)\rangle\propto\frac{2k_BT}{Kq^2+C\xi_+^{-1}}e^{-t[(K/\eta)q^2+C'\xi_+^{-1}]}\ , \tag{2.7}$$

where η is a 2D viscosity and C and C' are constants. For the Sm-C regime, the ξ_+^{-1} terms go to zero and one recovers the spin-wave limit. At some temperature above $T_{C\text{-}A}$ these q-independent correction terms become important; this will occur for ~ 20 mK above $T_{C\text{-}A}$ for $q\simeq 1000$ cm^{-1} in the material DOBAMBC.[15] This dependence of the scattered intensity $I(q,t)$ and decay time τ_d on ξ_+ and hence on reduced temperature is peculiar to the KT aspects of the transition,

$$1/\tau_d\propto\frac{K}{\eta}q^2+C'\xi_+^{-1}\ , \tag{2.8a}$$

$$1/I(q)\propto Kq^2+C\xi_+^{-1}\ . \tag{2.8b}$$

In the Sm-A phase, for $K=0$ the decay time and intensity go to zero roughly as ξ_+. The bracketed terms in Eq. (2.6) do not rescale the values of K or η near $T_{C\text{-}A}$. Simi-

larly, in the limits of Sm-A-like behavior, the second and third terms within the square brackets of Eq. (2.6) evaluate to exponential decays multiplied by slowly varying functions of time. This results in the electric field autocorrelation function having the form

$$\langle E_s(q,t)E_s^*(q,0)\rangle \simeq e^{-tA\xi_+^{-1}}, \tag{2.9}$$

where A is a constant. Thus, even above $T_{C\text{-}A}$, there are Sm-C-like fluctuations, but their decay time varies as ξ_+ and hence falls rapidly to zero with increasing temperature.

III. EXPERIMENTAL TECHNIQUE

Measurements were made as a function of temperature on thin, freely suspended films of the ferroelectric liquid-crystal DOBAMBC (see Fig. 1).[16] Proton NMR spectra taken on the samples discussed here put an upper bound of 0.25 wt. % on the amount of hydrocarbon impurities present. Freely suspended films were prepared as described previously[10] by drawing the liquid crystal over a 0.315 cm×0.8 cm hole in a glass coverslip and permitting the film to thin to a uniform thickness. An electric field of ~6 V/cm in the plane of the film was used to align the tilt and ensure a single-domain sample of the ferroelectric liquid crystal. The films were then inspected by eye through a 25× telescope for orientational defects. They were maintained in a two-stage oven with temperature stability of ~1 mK over the time scale of the measurements discussed here (about half an hour per temperature); dry nitrogen was flowed through the oven to prevent degradation of the liquid crystal. The resolution in reduced temperature was limited to ~10 mK by gradients in the film oven, while the measured hysteresis of the Sm-C to Sm-A transitions for the samples discussed here was ≤10 mK. Drifts in the transition temperatures were measured and compensated for in computing the reduced temperature; typical values were −8.5 mK/h for the ellipsometry measurements, and ~−0.2 mK/h for the light-scattering measurements. (The ellipsometry experiments necessitated cutting small slits open to the environment in the oven windows, while the light-scattering results were obtained with a sealed oven, and hence a more stable environment.)

The experimental apparatus, inspired by previous ellipsometry measurements on liquid crystals,[12,17] is shown in Figs. 2(a) and 2(b). Slight modifications in the design of the apparatus allow either ellipsometry or light-scattering measurements to be taken on the same film. The ellipsometer used was in the polarizer-compensator-sample-analyzer (PCSA) configuration.[18] While the accuracy of the measured phase shifts was limited to 0.01°, the precision of phase shift differences was ±0.003° and this was the limiting factor in the measurement of θ. For the ellipsometry measurements, the phase shift of the films in the Sm-A phase was used to determine the thicknesses. For the light-scattering measurements, thicknesses were determined from the intensity of light reflected from the films.

The ellipsometry data were fitted by assuming that the films could be modeled as a single uniform slab and treated using the matrix method for stratified media to compute the relevant polarization shifts as a function of θ.[19] The values used for the extraordinary and ordinary indices of refraction of DOBAMBC, measured by Garoff in bulk samples, are $n_e = 1.705 \pm 0.005$ and $n_o = 1.478 \pm 0.002$.[20] Since θ should correspond to the angle that the optical axis makes with the normal to the film and the aligning electric field fixes the tilt direction, the director orientation completes the specification of the

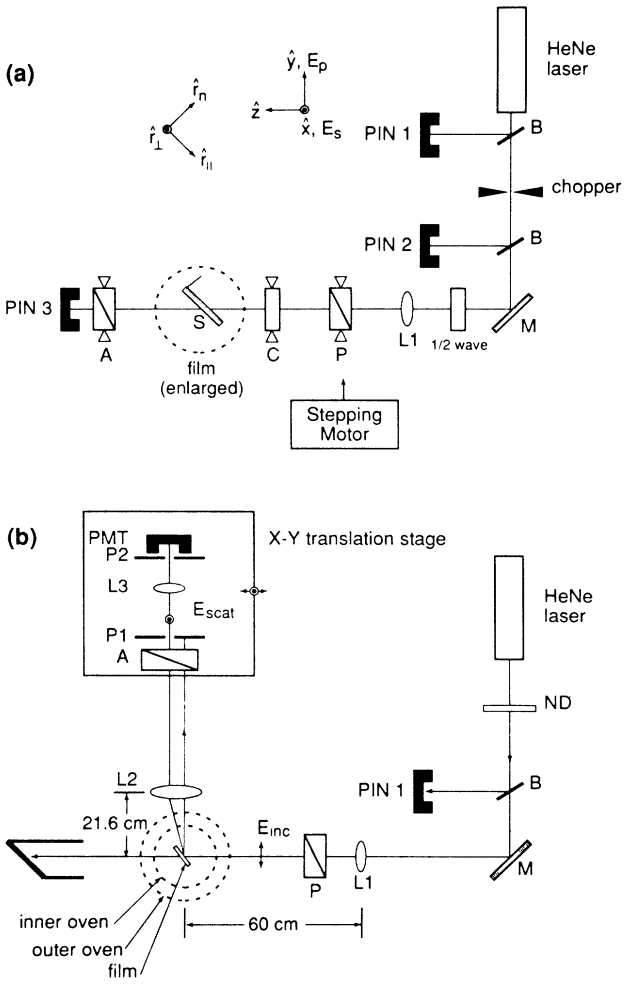

FIG. 2. (a) Schematic diagram of the PCSA ellipsometer. The film (S) is oriented with its normal at 45° to the incident beam. The polarizer, P, is rotated by computer-controlled stepping motors during a scan. The compensator C is fixed and the analyzer A is adjusted for a null at the beginning of each set of scans. The other optical components are lenses (L1 and L2), a mirror (M), beamsplitters (B), neutral density filters (ND), and photodiode detectors (PIN). The spatial filter-detector assembler consists of the photomultiplier tube (PMT), lense (L2), and spatial filter pinholes P1 and P2. (b) Schematic diagram of the light-scattering experiment. The scattered light is measured in a reflection geometry and scans in 2D momentum transfer are accomplished by translating the detector on an XY stage. All the optical elements within the x-y translation stage area are translated as a unit at all times.

dielectric tensor. With n_e and n_o known, only one value of polarizer angle sufficed to determine $\langle\theta\rangle$, the value of θ averaged over the layers of the film, for a given temperature.[21] These assumptions gave excellent fits to the measured data for all thicknesses and temperatures. The effects of fluctuations in ϕ will reduce the measured value of $\langle\theta\rangle$; this corresponds to the effects of vortices on the effective elastic constants, and hence $\langle\theta\rangle$, close to $T_{C\text{-}A}$ in the KT theory.

Figure 3 shows a summary of tilt data taken for films three, four, five, six, and eleven molecular layers thick with a temperature resolution of 15 mK. The general shape of the curves for all thickness films agree: far away from the critical region, there is a gradual, approximately linear, falloff in $\langle\theta\rangle$ as the temperature approaches $T_{C\text{-}A}$ from below, while close to the transition, there is a break in slope of the $\langle\theta\rangle$ curve above which $\langle\theta\rangle$ falls off rapidly to zero. As previously observed, the transition temperature is a strong function of film thickness; the possibility of nonuniformity of the tilt profile across the film thickness is indicated by the fact that, for the same reduced temperature, the value of $\langle\theta\rangle$ grows smaller as the thickness of the film under consideration increases.[12] In a three-dimensional system, the critical temperature $T_{C\text{-}A}$ would be assumed to correspond to the point at which $\langle\theta\rangle$ goes to zero after the expected smooth, monotonic decrease with increasing temperature. In thin films, the situation can be more complex because of the more complex shape of the transition region and the nonuniformity in the tilt profile across the film.

In explaining these phenomena, we first considered the two simplest situations which could possibly arise: either every layer has the same value of tilt at the same temperature, in which case $\langle\theta\rangle$ is independent of N; or only a subset of the layers are tilted with the other layers remaining upright and effectively Sm-A. The observed dependence of $\langle\theta\rangle$ upon N for a fixed reduced temperature refutes the first hypothesis. In actuality, we find that when their critical regions are shifted to coincide, one can choose an arbitrary multiplicative factor $f(N)$ such that when the average tilts for each N are scaled by $f(N)$, the data overlap exactly over a region within at least 5 °C of the transition (see Fig. 4). We interpret this observation in the following fashion: if only the surface layers were ordered very close to the Sm-C to Sm-A transition, then the average value of the tilt would vary as $\langle\theta(N)\rangle = 2\theta_s/N$, where θ_s is the tilt angle of the two surface monolayers. Hence the average tilts $\langle\theta(N)\rangle$ for different thickness films should vary according to the same functional form as any given thickness $\langle\theta(3)\rangle$, for example, when multiplied by $f(N) = \langle\theta(3)\rangle / \langle\theta(N)\rangle = N/3$. This prediction for $f(N)$ is plotted along with the actual measured scaling factors in the inset to Fig. 4. The agreement is quite good, leading to the con-

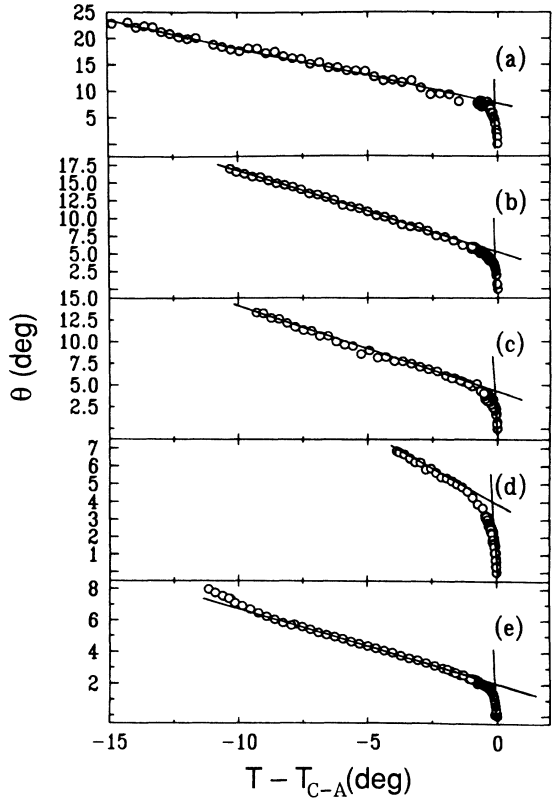

FIG. 3. Values for the average tilt across the film profile $\langle\theta\rangle$ as a function of temperature for films three, four, five, six, and eleven layers thick, (a)–(e), respectively. The method for obtaining the values of θ^* is indicated. Straight lines were drawn through the tilt data for values of temperature above and below the kink in the tilt data, and their intersection used as a measure of the jump in the data. The results of this process are given in Table I.

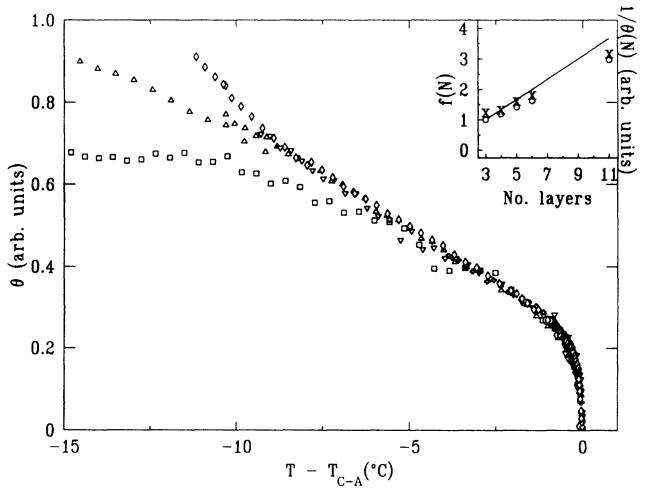

FIG. 4. Data for θ scaled by a factor $f(N)$ for each N layer film so that the tilts near $T - T_{C\text{-}A} = 0$ are independent of film thickness. The data symbols represent the following: three layers (open squares), four layers (open upright triangles), five layers (open inverted triangles), six layers (crosses), seven layers (stars), and eleven layers (diamonds). Inset: Dependence of $f(N)$ (circles) upon N. The values of $1/\theta(N)$ for $T - T_{C\text{-}A} = -3.877$ °C (crosses), scaled by a multiplicative constant to overlap with the $f(N)$ data, are also included, while the straight line shows the result expected if each film had only two tilted layers.

clusion that for a range of temperatures close to the transition, it is appropriate to treat the system as two Sm-C monolayers on a Sm-A bulk film. Thus the strongest version of surface-enhanced ordering holds, and any effects due to enhanced, exponentially decaying tilt order in the interior layers of the films are negligible close to the transition.[12] If the Sm-A interior layers were to completely screen the surface monolayers from each other, then this system would be an exact realization of the 2D XY system. The discussion presented below indicates the degree of interaction that actually exists between opposite surfaces.

We will now discuss the critical behavior of the monolayer Sm-C—Sm-A transition. Within approximately 0.1 °C of the temperature at which the tilt goes to zero, each set of data shows a significant change in slope of $\langle\theta\rangle$, above which the tilt goes very abruptly to zero (Fig. 3). In the data shown in Fig. 4, this feature of the data has the same shape and position for each thickness film studied when the transition temperatures were shifted to coincide. We believe that this abrupt jump to zero represents the universal jump to zero predicted by Nelson and Kosterlitz for the XY model.[13] We argue that the tilted surface monolayers undergo an XY transition, with the position in temperature of the break in slope corresponding to $T_{C\text{-}A}$ and the value of $\langle\theta\rangle$ at this temperature corresponding to θ^*. This possibility had been raised earlier by Rosenblatt *et al.*[10] and Heinekamp *et al.*[12] The finite falloff of $\langle\theta\rangle$ above this curve due to rounding of the transition is possibly due to the temperature inhomogeneities discussed above. If this hypothesis is correct, then the size of the jump in θ for each monolayer should be independent of film thickness. The size of the jump was measured using the simple graphical procedure, illustrated in Fig. 3: a line was drawn through the values of $\langle\theta\rangle$ far below $T_{C\text{-}A}$, where the tilt scales approximately linearly with temperature. The steep part of the curve above the kink in temperature was also fitted to a line and the intersection of these two lines was used as the value of θ^*. Table I shows that when the jump in $\langle\theta(N)\rangle$ is scaled by $N/2$ to obtain the monolayer jump value θ_s^*, then the same value is obtained for each value of N to within the error bars: $\theta_s^* = 11° \pm 1°$. Equation (2.5) can be used to extract values for the bulk elastic constant from the prediction for θ^*; the values derived are $K_{11} = 1.4 \times 10^{-6}$ dyn, in good agreement with values of K_{11} derived from previous bulk measurements and light-scattering data.[10,22]

TABLE I. Results of the computation of the jump in θ measured at $T_{C\text{-}A}$ as a function of thickness. The values of θ^* correspond to the numbers obtained from Fig. 3 by the procedure described in the text. The values of $\theta^* N/2$, consequently, are the measurements of the monolayer universal jump in θ.

Number of layers	θ^* (deg)	$\theta^* N/2$ (deg)
3	7.5	11
4	5.0	10
5	4.1	10
6	3.8	11
11	2.0	11

Since $T_{C\text{-}A}$ depends strongly upon N,[12] layer-layer interactions must play a strong role in the transition, unlike the case of monolayer freezing.[23] This is also manifested in the eventual departure of $\langle\theta\rangle$ from the rule $\langle\theta\rangle = 2\theta_s/N$.[12] Indeed, when the films were lowered in temperature toward the Sm-I phase, the average values of the tilt gradually approached the same values independent of N, eventually reaching the bulk saturation value of 30° at the Sm-C to Sm-I transition, as shown in Fig. 5. The picture that emerges has the two surface layer tilts growing for $T \leq T_{XY}$, after which successive interior layers gradually tilt also. This case resembles critical wetting, with the Sm-C tilt nucleating from the surface and gradually spreading into the interior of the film. This leads us to believe that the Sm-C to Sm-A transition proceeds via a novel wetting phenomena whereby over a fairly extended range in temperature *only* surface layers are ordered, with the ordering in additional layers setting in gradually as the temperature is lowered. Data for two- and four-layer films taken over the entire range of the Sm-C phase corresponded well to fits using the mean-field theory proposed by Dumrongrattana *et al.* for the bulk Sm-C to Sm-A transition[24] (see Fig. 5). The analysis of Heinekamp *et al.*[12] of films two layers and thicker showed that, except for the region nearest to the Sm-C to Sm-A transition, a mean-field theory with effects due to enhanced surface tilts accounts qualitatively for the main features of the $\langle\theta\rangle$ data. In particular, their model reproduces the dependence of $T_{C\text{-}A}$ on the number of layers N. However, this model does not give the scaling of $\langle\theta\rangle$ with N over the observed temperature range shown in Fig. 4, so a complete description of the wetting behavior remains to be found.

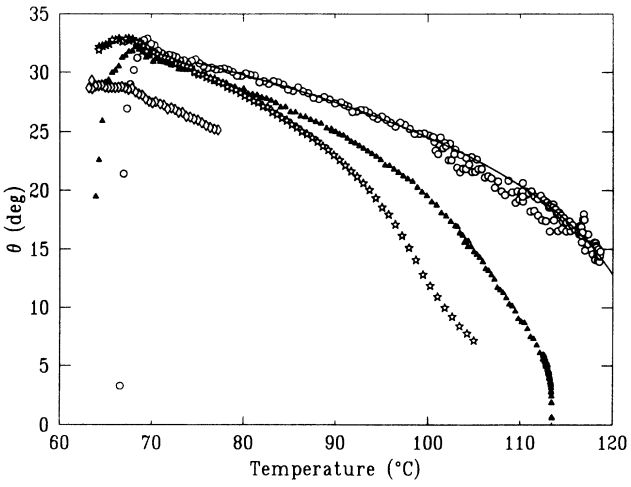

FIG. 5. Ellipsometry data for $\langle\theta\rangle$ near $T_{C\text{-}I}$ for two-layer (open circles), four-layer (closed triangles), seven-layer (stars), and eleven-layer (diamonds) films. The peak in the til angle for each thickness corresponds to the Sm-C–Sm-I transition. The results of a mean-field theory fit (solid line) for the two-layer data over the temperature range shown show that the tilt never saturates before the Sm-C–Sm-I transition.

To further characterize the phase transition, light-scattering measurements were also performed on thin films, two, three, four, and five layers thick. The scattering geometry was such that by scanning the detector in the x-y plane, one could probe different directions in the 2D momentum-transfer vector $\mathbf{q}$. The data described here were taken for a range of momentum transfer covering $1000\ \text{cm}^{-1} \leq |q_{\parallel}| \leq 4000\ \text{cm}^{-1}$ and $2000\ \text{cm}^{-1} \leq |q_{\perp}| \leq 4000\ \text{cm}^{-1}$. From the light-scattering data taken as a function of $q_{\perp,\parallel}$, the average intensities and decay times, and hence the 2D elastic constants, $K_{\perp,\parallel}$ and 2D viscosities, $\eta_{\perp,\parallel}$, could be derived using Eq. (2.7).

The basic physics observed can be shown by first examining the behavior of the average intensity $\langle I(q) \rangle$ and decay time τ_d taken at a fixed value of $\mathbf{q}$ as a function of temperature. This is shown in Fig. 6 for a four-layer film. Two temperature effects are noticeable here: within the Sm-C phase, τ_d is roughly constant [see Fig. 6(b)], rising to a weak peak $\sim 30\%$ higher than the value of 2.0×10^{-3} sec at 112.96 °C and finally falling steeply off to zero at 113.07 °C. The intensity [Fig. 6(a)] falls off approximately linearly as T approaches $T_{C\text{-}A}$, with an abrupt break in slope at $T_{C\text{-}A} = 112.96$ °C, falling abruptly to a small but constant value at roughly 113.07 °C. (The location of the actual transition temperature will be discussed below.) These events are consistent with the expected physics based on the previously mentioned model. As the temperature is increased close to $T_{C\text{-}A}$, there is a weak slowing down of the fluctuations in azimuthal angle, corresponding to the peak in τ_d; the intensity decreases because, while the fluctuations are becoming more highly correlated, the overall factor of $\sin^2\theta$ in the expression for the scattered intensity is becoming smaller due to the decrease in θ. This behavior was seen at all values of $\mathbf{q}$ probed. All DOBAMBC samples used exhibited these effects for every measurement obtained in this fashion, with roughly the same widths of the region between the two temperature anomalies for every film.

Our identification of $T_{C\text{-}A}$ as the temperature at which the kink in intensity and weak peak in τ_d appear relies upon a comparison of the results of ellipsometry and light-scattering measurements on the same film. This was difficult to do in the geometry described above, so a slightly modified geometry, the polarizer-sample-compensator-analyzer configuration was employed.[18] The light-scattering experiment was either set up after an ellipsometry measurement had been obtained and performed on the same film, as for the data shown in Fig. 7, or the intensity autocorrelation functions were monitored while the polarization data was being measured to pinpoint where the peak in τ_d and the disappearance of the decaying exponentials occurred. The results for these two techniques are shown in Fig. 7. The midpoint of the region in which the polarizer angle $P \propto \theta$ goes to zero corresponds closely to the temperature where τ_d becomes unmeasurably small. The peak in τ_d and the kink in intensity correspond to the same temperature as the abrupt change in slope in θ noted earlier, and ascribed to the universal jump in θ at $T_{C\text{-}A}$.

To see if the shape of the transition region was a field-dependent effect we studied the effect of the aligning field by taking data for a single film at three different field strengths: 6.35 V/cm, the usual value, and for fields one-half and one-fourth that value. The data taken near $T_{C\text{-}A}$ all had the same functional dependence upon temperature for all three values of the aligning field used. No extra rounding was observed near the transition as a result of increasing the field strength. Similarly, since the light-scattering data have the same form for films three,

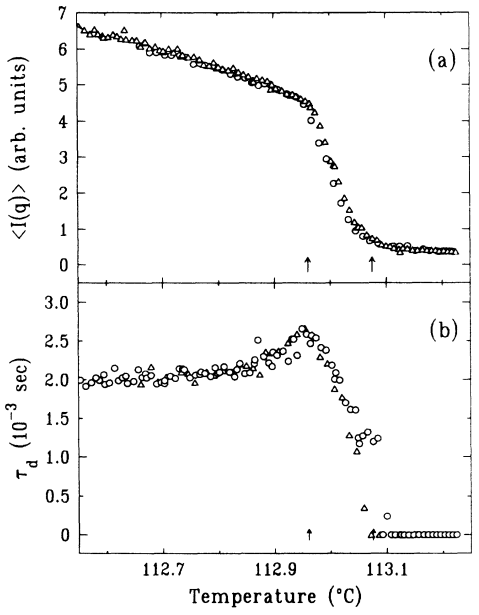

FIG. 6. Scans taken at fixed $q_{\parallel} = 1976.6\ \text{cm}^{-1}$ on a four-layer film with approximately 10-mK temperature steps on cooling (triangles) and approximately 5-mK temperature steps on heating (circles) near the transition. The two curves differ only in that the values of τ_d very close to $T_{C\text{-}A}$ are better resolved for the cooling data. The arrows indicate $T_{C\text{-}A}$ at 112.96 °C.

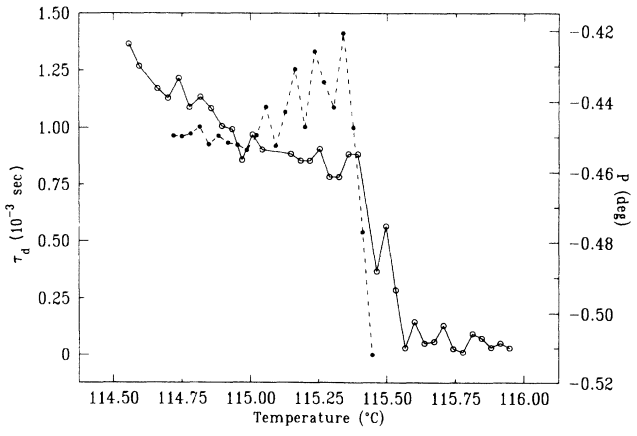

FIG. 7. Light-scattering and ellipsometry data taken in successive heating runs upon the same three-layer film. Plotted are the decay times τ_d at fixed $q_{\perp}$ (closed circles) and the polarizer angle $P \propto \theta$ (open circles) as a function of temperature near the Sm-C to Sm-A transition.

four, and five layers thick when scaled by a multiplicative factor, we do not believe the shape of the transition region can be attributed to film thickness.

Using the suitable form of Eq. (2.7), the intensity and decay time data as a function of $\mathbf{q}$ could be analyzed to provide the dependence of $K_{\parallel}$, $K_{\perp}$, and the 2D diffusion constants $K_{\perp}/\eta_{\perp}$ and $K_{\parallel}/\eta_{\parallel}$ (Fig. 8); the values of the latter permit determination of the 2D viscosities as well. These material constants are predicted to decrease as the temperature is increased towards $T_{C\text{-}A}$ as $\sin^2\theta$ [see Eq. (2.4)]. As demonstrated by Fig. 8, the derived values of $K_{\perp}$ and $K_{\parallel}$ do indeed have the expected scaling property with respect to θ, confirming the predictions of the theory in spite of the nonuniform tilt profile across the film.

Our attempts to measure the universal jump in the 2D elastic constants were hindered by the fact that, since Sm-C fluctuations were visible throughout the entire region where $\theta \neq 0°$, it was always possible to attempt to fit a value of K to the observed data, making it impossible to assign a lower limit on the universal jump in K. As the temperature was raised above what we have here called $T_{C\text{-}A}$, weak Sm-C fluctuations persisted with progressively weaker dependence upon $\mathbf{q}$. Thus the smallest values measured for $K_{\perp}$ and $K_{\parallel}$ correspond to the last values at which good fits could be obtained rather than to a discontinuous jump in the elastic constants, so that, unfortunately, we were not able to correlate a jump in $K_{\perp}$ or $K_{\parallel}$ with that observed in $\langle\theta\rangle$. However, as will be discussed below, this behavior of the light-scattering data is still consistent with the interpretation of the tilt data in terms of a universal jump in θ at $T_{C\text{-}A}$ as described earlier, and with theoretical predictions for the transition.

The observed features of the Sm-C to Sm-A transition appear to be described by the dynamical theory of Heinekamp and Pelcovits.[15] The crossover point in temperature they predict for which the dependences of the intensity and decay time on reduced temperature changes radically represents the effective XY transition temperature for the measurement and so might be conjectured to correspond to what has here been called $T_{C\text{-}A}$. Above this crossover point, the system will effectively be in the Sm-A phase, even though correlated light scattering from fluctuations in the director persists indefinitely high in temperature, so that, as has been measured here, there is no single point at which fluctuations disappear altogether. Above the effective $T_{C\text{-}A}$, the intensity autocorrelation functions will still be singly decaying exponentials, but the intensity and decay times will fall off as ξ_+ with $b \simeq (2\,°\text{C})^{1/2}$ [see Eqs. (2.1) and (2.7)]; both quantities will cease to depend upon $\mathbf{q}$ at some point above $T_{C\text{-}A}$, again in agreement with the measurements. The test of these predictions is demonstrated in Fig. 9, which shows the re-

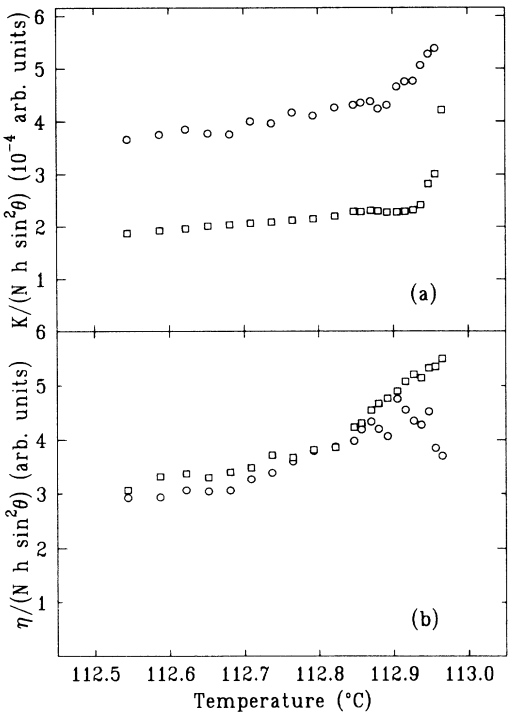

FIG. 8. Comparison of the scaling of the elastic constants and viscosities with $\sin^2\theta$ for the perpendicular (circles) and parallel (squares) modes. (a) The ratio for the elastic constants $K/(Nh\sin^2\theta)$. For the perpendicular mode this should correspond to the bulk elastic constant K_{11}. (b) The ratio for the viscosities $\eta/(Nh\sin^2\theta)$.

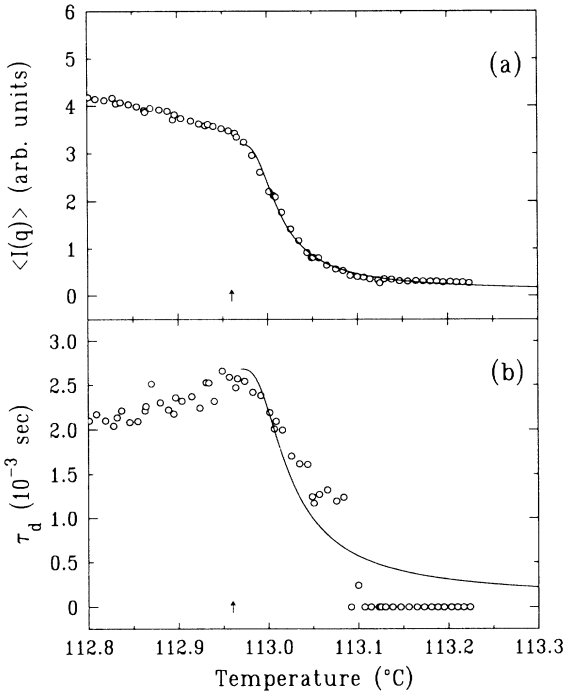

FIG. 9. Results of fitting the intensity and decay time for a fixed $\mathbf{q}$ to the functional form given in Eq. (3.1): (a) intensity (circles) and the best fit to the intensity data (solid line), which gives $b = 1.1$; (b) τ_d (circles) and the fit to the τ_d data (solid line) holding b at the same value as found for (a). The fit was performed holding $T_{C\text{-}A}$ at 112.965 and fitting for $T \geq 112.965\,°\text{C}$. Data points set exactly to zero had decay times too small to measure.

sults of fitting the intensity to the functional form

$$\frac{1}{e^{-b/|T-T_{C\text{-}A}|^{1/2}}+C}, \tag{3.1}$$

where C is some constant which cuts off the divergence in ξ_+ at $T_{C\text{-}A}$, with the transition temperature fixed at the temperature at which the anomaly occurs. As Fig. 9 shows, the agreement with the intensity data is quite good for $b \simeq 1.1\,^{\circ}\mathrm{C}^{1/2}$. The τ_d data were fitted with this value for b held fixed; they do not agree as well as the intensity data with this functional form, and the poor quality of the data above the anomaly make it impossible to obtain a meaningful fit to other values of b. The data presented here cover roughly an order of magnitude of reduced temperature and do not determine the exponent in Eq. (3.1) to better than 0.5 ± 0.1.

The predicted dependence of the observed, effective $T_{C\text{-}A}$ on $\mathbf{q}$ should not be evident in these data because the shift in the observed $T_{C\text{-}A}$ depends only logarithmically upon $\mathbf{q}$, and the measured values of $\mathbf{q}$ do not cover a wide enough range. The theory does indeed predict different transition temperatures for ellipsometry and light-scattering measurements made on the same film, since these probe different length scales (for light scattering $q \sim 2000\ \mathrm{cm}^{-1}$, while for ellipsometry the characteristic scale is $\sim 200\ \mu\mathrm{m}$, the illuminated area's diameter). From these values, one would expect $T_{C\text{-}A}$ from ellipsometry to be lower than that for light scattering by only ≤ 0.01 mK, a difference unresolvable by these measurements.

IV. CONCLUSIONS

The picture of two tilted Sm-C surface layers undergoing a 2D XY transition is consistent with both the ellipsometry and light-scattering observations presented here. These data present an especially nice confirmation of the Kosterlitz-Thouless melting theory, since the scaling of θ with N conclusively demonstrates that only the surface monolayers order and hence the system should truly represent a two-dimensional system. The values for the universal jump in the surface tilt at which the curves for θ abruptly go to zero agree for all thickness films measured and give predictions for the bulk elastic constants in agreement with other measurements on thin films and in bulk. This jump in θ coincides in temperature with anomalies in the light-scattering intensity and decay times predicted to accompany the 2D XY transition. The theoretical predictions of Heinekamp and Pelcovits for the behavior of the intensity and decay times characterizing light-scattering above $T_{C\text{-}A}$ agree well over about an order of magnitude of reduced temperature with the measured data; these predictions correspond intuitively to a crossover from scattering by fluctuations in ϕ to scattering by fluctuations in θ caused by the defect unbinding transition.

ACKNOWLEDGMENTS

This work was supported by National Science Foundation Grants No. NSF-85-13523 and No. NSF-DMR-86-14003 to the Harvard Materials Research Laboratory, as well as by the Joint Services Electronics Program Grant No. JSEP-N0001484-K-0465. Robert Pelcovits has spent a great deal of time discussing and extending his theories of the smectic-C to smectic-A transition in conversations with us, shaping much of the analysis presented here. We also benefited greatly from helpful conversations with David Nelson, Mark Schlossman, Eric Sirota, Larry Sorensen, and Sam Sprunt. Finally, we wish to thank Hans Biebuyck for his assistance in taking NMR spectra of the liquid-crystal samples studied here.

*Present address: Department of Chemistry, University of Pennsylvania, Philadelphia, PA 19104.

[1]J. M. Kosterlitz and D. J. Thouless, J. Phys. C **5**, L124 (1972); **6**, 1181 (1973); in *Progress in Low Temperature Physics,* edited by D. F. Brewer (North-Holland, Amsterdam, 1978), Vol. VII-B; J. Kosterlitz, J. Phys. C **7**, 1046 (1974).

[2]I. Rudnick, Phys. Rev. Lett. **40**, 1454 (1978).

[3]D. J. Bishop and J. D. Reppy, Phys. Rev. Lett. **40**, 1727 (1978).

[4]E. Webster, G. Webster, and M. Chester, Phys. Rev. Lett. **42**, 243 (1979).

[5]J. A. Roth, G. J. Jelatis, and J. D. Maynard, Phys. Rev. Lett. **44**, 333 (1980).

[6]For example, D. J. Resnick, J. C. Garland, J. T. Boyd, S. Shoemaker, and R. S. Newrock, Phys. Rev. Lett. **47**, 1542 (1981).

[7]See, for example, Y. Saito and H. Muller-Krumbharr, in *Applications of the Monte Carlo Method in Statistical Physics,* Vol. 36 of *Topics in Current Physics,* edited by K. Binder (Springer, New York, 1984); J. F. Fernandez, M. F. Ferreira, and J. Stankiewicz, Phys. Rev. B **34**, 292 (1986).

[8]C. Y. Young, R. Pindak, N. A. Clark, and R. B. Meyer, Phys. Rev. Lett. **40**, 773 (1978).

[9]C. Rosenblatt, R. Pindak, N. A. Clark, and R. B. Meyer, Phys. Rev. Lett. **42**, 1220 (1979).

[10]C. Rosenblatt, R. B. Meyer, R. Pindak, and N. A. Clark, Phys. Rev. A **21**, 140 (1980).

[11]C. Rosenblatt, Ph.D. thesis, Harvard University, 1976 (unpublished).

[12]S. Heinekamp, R. A. Pelcovits, E. Fontes, E. Yi Chen, R. Pindak, and R. B. Meyer, Phys. Rev. Lett. **52**, 1017 (1984).

[13]D. R. Nelson and J. M. Kosterlitz, Phys. Rev. Lett. **39**, 1201 (1977).

[14]R. A. Pelcovits and B. I. Halperin, Phys. Rev. A **19**, 4614 (1979).

[15]S. W. Heinekamp and R. A. Pelcovits, Phys. Rev. A **32**, 2506 (1985).

[16]R. B. Meyer, L. Liebert, L. Strzelecki, and P. Keller, J. Phys. (Paris) **36**, 69 (1975).

[17]Y. Galerne, Phys. Rev. A **24**, 2284 (1981); J. Phys. (Paris) **46**, 733 (1985).

[18]R. M. A. Azzam and N. M. Bashara, *Ellipsometry and Polarized Light* (North-Holland, Amsterdam, 1977).

[19]M. Born and E. Wolf, *Principles of Optics* (Pergamon, Oxford, 1980).

[20]S. Garoff, Ph.D. thesis, Harvard University, 1977 (unpublished).
[21]For other details of the ellipsometry and light-scattering measurements, see S. M. Amador, Ph.D. thesis, Harvard University, 1989.
[22]H. Takezoe, K. Kondo, K. Miyasato, S. Abe, T. Tsuchiya, A. Fukuda, and E. Kuze, Ferroelectrics **58**, 55 (1984).
[23]R. Pindak, D. J. Bishop, and W. O. Sprenger, Phys. Rev. Lett. **44**, 1461 (1980).
[24]S. Dumrongrattana, C. C. Huang, G. Nounesis, S. C. Lien, and J. M. Viner, Phys. Rev. A **34**, 5010 (1986).

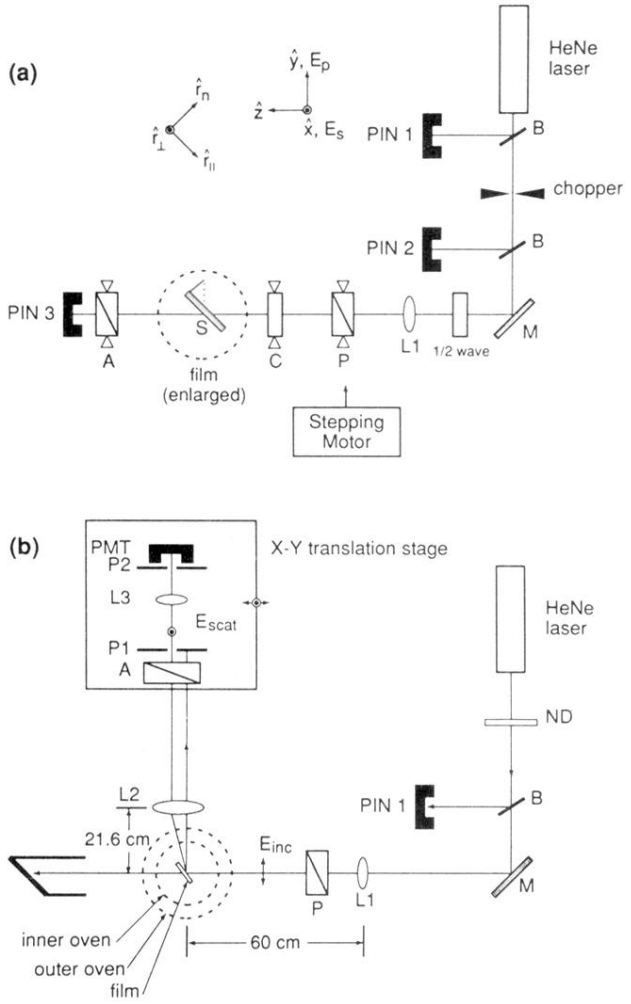

FIG. 2. (a) Schematic diagram of the PCSA ellipsometer. The film (S) is oriented with its normal at 45° to the incident beam. The polarizer, P, is rotated by computer-controlled stepping motors during a scan. The compensator C is fixed and the analyzer A is adjusted for a null at the beginning of each set of scans. The other optical components are lenses (L1 and L2), a mirror (M), beamsplitters (B), neutral density filters (ND), and photodiode detectors (PIN). The spatial filter-detector assembler consists of the photomultiplier tube (PMT), lense (L2), and spatial filter pinholes P1 and P2. (b) Schematic diagram of the light-scattering experiment. The scattered light is measured in a reflection geometry and scans in 2D momentum transfer are accomplished by translating the detector on an XY stage. All the optical elements within the x-y translation stage area are translated as a unit at all times.